Published in final edited form as:
Acta Biomater. 2012 January ; 8(1): 225–233. doi:10.1016/j.actbio.2011.08.001.

Mechanical Property Characterization of Electrospun Recombinant Human Tropoelastin for Vascular Graft Biomaterials

Kathryn A. McKenna[a,b], **Monica T. Hinds**[b,*], **Rebecca C. Sarao**[a], **Ping-Cheng Wu**[a], **Cheryl L. Maslen**[c], **Robert W. Glanville**[a], **Darcie Babcock**[c], and **Kenton W. Gregory**[a]

[a]Oregon Medical Laser Center, Providence St. Vincent Medical Center, 9205 SW Barnes Rd. Portland, Oregon, 97225

[b]Department of Biomedical Engineering, Oregon Health & Science University, 3303 SW Bond Ave, Mailcode: CH13B, Portland, Oregon, 97239

[c]Division of Cardiovascular Medicine, Oregon Health & Science University, 3303 SW Bond Ave, Mailcode: CH14B, Portland, Oregon, 97239

Abstract

The development of vascular grafts has focused on finding a biomaterial that is non-thrombogenic, minimizes intimal hyperplasia, matches the mechanical properties of native vessels and allows for regeneration of arterial tissue. In this study, the structural and mechanical properties and the vascular cell compatibility of electrospun recombinant human tropoelastin (rTE) were evaluated as a potential vascular graft support matrix. Disuccinimidyl suberate (DSS) was used to cross-link electrospun rTE fibers to produce a polymeric recombinant tropoelastin (prTE) matrix that is stable in aqueous environments. Tubular 1 cm diameter prTE samples were constructed for uniaxial tensile testing and 4 mm small-diameter prTE tubular scaffolds were produced for burst pressure and cell compatibility evaluations from 15 wt% rTE solutions. Uniaxial tensile tests demonstrated an average ultimate tensile strength (UTS) of 0.36±0.05 MPa and elastic moduli of 0.15±0.04 MPa and 0.91±0.16 MPa, which were comparable to extracted native elastin. Burst pressures of 485 ± 25 mmHg were obtained from 4 mm ID scaffolds with 453 ± 74 μm average wall thickness. prTE supported endothelial cell growth with typical endothelial cell cobblestone morphology after 48 hours in culture. Cross-linked electrospun recombinant human tropoelastin has promising properties for utilization as a vascular graft biomaterial with customizable dimensions, a compliant matrix, and vascular cell compatibility.

Keywords

Tropoelastin; Electrospinning; Mechanical properties; Vascular grafts; Tissue Engineering

>*Correspondence to: Monica T. Hinds, PhD, Associate Professor, Department of Biomedical Engineering, Oregon Health & Science University, 3303 SW Bond Ave., Mailcode: CH13B, Portland, OR 97239, hindsm@ohsu.edu, Tel.: 1-503-418-9309, Fax: 1-503-418-9311 .
kathryn.mckenna@providence.org (K. M.); hindsm@ohsu.edu (M. H.); rebecca.sarao@providence.org (R. S.); Ping-Cheng.Wu@providence.org (P. W.); maslenc@ohsu.edu (C. M.); robert.glanville@providence.org (R. G.); babcockd@ohsu.edu (D. B.); ken.gregory@providence.org (K. G.)

1. Introduction

Heart disease remains the leading cause of death in the Western world with nearly 81 million people affected in the United States in 2006 [1]. Bypass surgery using autografts of saphenous veins or mammary arteries remains the gold standard treatment for severe cases, but can be limited by previous vessel harvest or preexisting disease. Synthetic graft materials, such as expanded poly(tetrafluoroethylene) (ePTFE) and poly(ethylene terephthalate) (PET or Dacron®), work well for large diameter vessels, but are not viable options for grafts smaller than six millimeters in diameter [2].

The failure modes of small diameter vascular grafts have primarily been thrombosis, aneurysm, and intimal hyperplasia [3]. To address these failure modes many researchers have studied both synthetic and natural biomaterial scaffolds. Synthetic biomaterials have controllable physical and mechanical properties that are highly reproducible and are easily manufactured in large-scale quantities, but many lack the elasticity of native arteries and biocompatibility for long-term vascular cell functionality. Considerable efforts have been made to functionalize synthetic surfaces [4, 5]. Natural biomaterial scaffolds, including well-studied grafts of decellularized blood vessels [6-8], have had limited success. The decellularized bovine [6] and human [7] blood vessels had promising 5 year patency rates, yet aneurysm formation due to *in vivo* degradation limited their widespread use [7, 8]. Decellularized arteries, from allogenic and xenogenic sources are attractive scaffolds for tissue-engineered vascular grafts due to their mechanical and biological properties [9], yet these natural scaffolds are limited by the lack of precise manufacturing control of the physical and mechanical properties, as well as problems with inflammation and calcification [18]. To reduce concerns of inflammation of the allogenic and xenogenic sourced vascular biomaterials, the biomaterials are frequently cross-linked; yet this has led to problems of limited cell repopulation and increased stiffness of the biomaterials [19]. While stiffness and compliance mismatch alone may not lead to vascular graft failure [27-29], graft compliance has correlated to the formation of intimal hyperplasia and should be considered in biomaterial scaffold design along with the potential of cellular remodeling of the graft and cell signaling capability [20-26]. The search for a viable off-the-shelf small diameter vascular graft that can match an autograft's performance in terms of mechanical properties, cell compatibility, and vascular healing has been the focus of many research efforts, but has remained an elusive target.

The incorporation of vascular cells with biomaterial scaffolds to produce tissue engineered grafts have been successful in animal and, recently, human trials [10-15]. Production of the scaffold by the vascular cells has been accomplished using both *in vivo* [11,16-17] and *in vitro* [12,13] methods. The *in vivo* methods require the graft to be grown in the recipient's peritoneal cavity. Recent advancements of this technique include improved scaffold design to produce multilayered scaffolds and the use of cyclic stretch to improve the assembly time and organization of the extracellular matrix [16,17]. Yet these *in vivo* methods require a second surgical site for autologous use. The *in vitro* methods of L'Heureux et al., where the tissue-engineered vascular grafts were produced from autologous cells without a scaffold, have advanced to clinical trails using an arteriovenous shunt model [12, 13]. These autologous tissue-engineered grafts have promising results with primary patency rates of 78% at 1 month and 60% at 6 months and the limited failures due to thrombosis, dilation, and aneurysm [12]. The *in vitro* cell produced scaffolds are elegant in design, but require lengthy production times potentially limiting their clinical use.

The use of electrospinning to make biomaterials has the capability of combining natural proteins with controllable physical and mechanical properties. Electrospinning produces submicron sized fibers from suspensions of monomers or polymers from both natural

proteins and synthetic polymers [30-34]. Fibers produced from monomer suspensions can then be cross-linked to produce stable polymeric structures with customizable dimensions in terms of fiber diameter and overall graft dimensions. Electrospun fibrous scaffolds made from biodegradable polymers, such as poly(-caprolactone) (PCL), polylactic acid (PLA), polyglycolic acid (PGA), and poly(lactide-co-glycolide) (PLGA) [35-38] have been proposed for use in bone, cardiac, blood vessel, and wound dressing applications [39-45]. Several groups have successfully electrospun elastin for use in tissue-engineered grafts [46-52] and support material for vein grafts [53]. Most, however, have used animal sourced elastin that is [20, 54-56] extracted from already assembled and cross-linked protein forms. While these forms of elastin may provide the biochemical signaling of elastin, they remain an animal sourced material with the associated potential for immuno-rejection leading to structural degradation and ultimate aneurismal graft failure.

Our aim is to electrospin small diameter vascular grafts containing recombinant human tropoelastin, the monomer unit of elastin, that when cross-linked mimics native elastin fibers. Elastin is the principal structural component of elastic arteries responsible for energy storage and recovery, and contributes to their unique mechanical properties [60]. End stage aneurysm disease and supravalvular aortic stenosis have been associated with the pathologic loss of elastin or deficiency in elastin expression [61-68]. Elastin, as a blood-contacting surface on stents and grafts, reduced thrombus adherence and demonstrated good long-term patency [69, 70]. Establishing an elastic fiber structure in a vascular scaffold that is similar to the arterial wall has been well recognized, as the depletion or loss of elastin has been correlated to both aneurysmal progression and severe smooth muscle cell hyperplasia in both animals and humans.[61, 64, 65, 67, 70, 82-84]. Thus, elastin is a promising, and perhaps necessary, component in vascular graft development [71, 72]. Recent work has examined a class of elastin-like recombinant polymers with self-assembly properties and cross-link sites designed into the peptide sequence [57]. The elastin-like polymer has been used to produce organized multilayer collagen reinforced vascular grafts and abdominal wall repair tissue constructs with customizable mechanical properties, which make this technology promising for many soft tissue applications [58, 59]. Our use of electrospinning will enable the customization of the dimensions and mechanical properties for the vascular graft biomaterial, and the use of tropoelastin may impart critical cell signaling to the biomaterial.

2. Materials and Methods

2.1. Materials

Human tropoelastin was optimized and expressed from a synthetic gene codon in gram quantities in a 10-liter *E.coli* fermentation system. Gel electrophoresis determined that the purification procedure resulted in a greater than 99% pure product (Figure 1) as well as low endotoxin levels with an average of 0.2 EU/mg (1 EU = 100 pg of endotoxin) as determined by the Kinetic-QCL Assay (Cambrex). All chemical reagents were acquired from Sigma-Aldrich unless otherwise noted.

The purified human tropoelastin protein includes all of the functional exons with the exception of exons 1, 22, and 26A (Figure 2). Exon 1 contains the signal sequence, while hydrophobic exon 22, and hydrophilic exon 26A are rarely expressed in mature elastin. The resultant tropoelastin exon structure used is the same as a natural isoform produced by normal human fetal heart cells.

Extracted porcine elastin was isolated as previously described [69]. Briefly, porcine carotid arteries were obtained from domestic swine of 250 lb and 6–9 months of age (Animal Technologies, Tyler, TX) to size match the diameters. The arteries were shipped overnight

in phosphate-buffered saline (PBS) on ice. The gross fat was dissected away and, using aseptic techniques, the arteries were placed in 80% ethanol for a minimum of 72 h at 4°C and subsequently treated with 0.25M NaOH for 70 min with sonication at 60°C, followed by two 30-min, 4°C washes in 0.05M HEPES (pH 7.4). The extracted elastin tubular conduits were then autoclaved at 121°C for 15 min and stored at 4°C in 0.05M HEPES buffer.

2.2 Electrospinning of rTE

Tropoelastin solutions of 15 wt% rTE in 1,1,1,3,3,3-hexafluro-2-propanol (HFP) were prepared and loaded into 2 or 5 mL glass syringes depending on the volume needed for each application. 18-gage stainless steel blunt tip needles were connected to the syringes and electrically coupled to a high voltage power supply (Glassman High Voltage, Inc., High Bridge NJ). A gap distance of 12.5 cm was set from the end of the needle to the center of the collection device. A syringe pump (Harvard Apparatus) was used to advance the protein solution at 2 mL/hr to refresh the solution at the tip of the syringe needle. Fibers were spun onto mandrels of either 1 cm diameter copper tubes for mechanical testing or 4 mm diameter stainless steel rods for small diameter graft production. Mandrels were connected to ground to complete the circuit. The collection system was set to rotate at 4400 rpm and translate longitudinally 6-8 cm with a rate of 8 cm/sec driven by a custom-built device with separate drives for longitudinal and rotational control. The solution was charged to an 18.5 kV excitation potential. All electrospinning was conducted within a chemical fume hood.

2.3. Cross-linking of Electrospun rTE

Disuccinimidyl suberate, DSS, (Pierce Biotechnology-Thermo Fisher Scientific Inc.), an organic amide bond cross-linker, was used to link electrospun rTE monomers to produce polymeric tropoelastin, prTE. Cross-linking was performed in a two-stage process. The electrospun rTE samples were incubated for 4 hours in DSS suspended in 50 mL anhydrous ethyl acetate, at a ratio of 0.072 mg of DSS per mg of rTE protein at room temperature in glass tubes. A second incubation occurred for 12-18 hours at a concentration of 0.108 mg of DSS per mg of rTE protein at room temperature. prTE samples were then rinsed in anhydrous ethyl acetate for 5 minutes with a second 5 minute rinse in 70% ethanol and a final 10 minute rinse in DI water. Final products were stored in 70% ethanol.

2.4. Electrospun rTE Fiber Characterization

The tubular scaffolds electrospun from 15 wt% prTE were analyzed with electron microscopy to determine fiber diameters and evaluate the degree of fiber orientation and consistency through the thickness of the graft. Electrospun prTE samples were mounted onto scanning electron microscopy (SEM) stubs and sputter-coated with 250 Å of gold/palladium. Micrographs were taken at magnifications from 3000 to 5000X and viewed at 5 kV on an FEI Sirion XL30 SEM. Image analysis of fibers was done with a custom MATLAB® program (MathWorks®) using a Laplacian edge detection algorithm followed by a Radon transform to determine the probability distribution of fiber orientation angles relative to horizontal.

2.5. Mechanical Properties of prTE

The mechanical properties of electrospun prTE samples were compared to extracted porcine elastin and native porcine carotid arteries. All uniaxial tensile tests were conducted on dogbone shaped specimens with a gage length of 10 mm and 4 mm grip ends. The tubular 1 cm diameter prTE samples were opened longitudinally, laid flat, and cut with a dye cutter. Four circumferential and four longitudinal sections were cut from each of the three electrospun samples. Eight longitudinal and eight circumferential samples were tested for native carotid arteries and extracted elastin conduits. All specimens were rehydrated in PBS

for at least 15 minutes prior to testing. The thickness, width, and gage length were recorded. The samples were mounted on custom tensile grips on a Chatillon Vitrodyne V1000 system with a 500 gram load cell or on a MTS 858 Mini Bionix II mechanical tester with a 5 lb load cell using spring action grips. All dogbone prTE samples were tested in tension at room temperature with a crosshead speed of 2 mm/sec until failure. Force and displacement measurements were acquired at 0.1 sec intervals. Engineering stress (force/cross-sectional area, F/A_{cs}) and strain (change in length/original length, L/L_o) were calculated and plotted. Linear regression of the slope in the stress-strain plots was used to calculate the elastic modulus (stress/strain, /). Elastic modulus 1 was measured between 10 and 30% strain, while elastic modulus 2 was measured between the maximum strain minus 20% and the maximum strain with linear curve fits to these regions of the stress strain curve. Peak stress (MPa) and strain (%) were taken as ultimate tensile strength (UTS) and percent elongation (ultimate strain). Compliance measurements were calculated using the stress and strain data between 50 and 100 kPA. Calculated values were based on the ANSI/ISO 7148 standard for "Cardiovascular implants – tubular vascular prostheses" [73]. Radius values at these stress values were calculated using a thin-walled cylinder approximation relating pressure to stress scaled by wall thickness and initial radius (Equation 1). Compliance was measured as the change in radius relative to the initial radius over the change in pressure or stress at 100 kPA and 50 kPa for each material (Equation 2).

$$\sigma_{\theta\theta}=\frac{P_i r_i}{t} \qquad \text{Equation 1}$$

$$\frac{\%compliance}{100mmHg}=\frac{\frac{R_2-R_1}{R_1}}{P_2-P_1}*10^4 \qquad \text{Equation 2}$$

Where = circumferential Cauchy stress, P = pressure, t = wall thickness, r = radius, R_2 = radius at P_2, and R_1 = radius at P_1.

2.6. Burst Pressure of prTE Scaffolds

Three 4 mm inner diameter, 5 cm long electrospun prTE scaffolds were fabricated for burst pressure analysis. Scaffolds of rTE were electrospun, cross-linked and stored in 70% ethanol prior to analysis. Wall thickness was measured using handheld digital micrometers and recorded. Scaffolds were cannulated onto barbed nylon connectors and secured using cotton umbilical tape. Samples were rehydrated in PBS for at least 30 minutes prior to testing. The ends of the scaffolds were fixed in position under zero longitudinal strain/load and saline was subsequently infused at a rate of 100 mL/min until failure occurred. The pressure (mmHg) was continuously monitored by an inline pressure transducer (Cole Parmer) and recorded with a custom built LabVIEW (National Instruments) data acquisition program.

2.7. Endothelial Cell Growth on prTE Scaffolds

Porcine bone marrow derived endothelial outgrowth cells (BMEOCs) were isolated and used to assess the growth of vascular cells on the lumenal surface of electrospun prTE vascular grafts. Porcine bone marrow mononuclear cells were collected and separated as previously reported [74]. Isolated cells were differentiated into BMEOCs in endothelial cell growth media (EGM2) at 37 C and 5% CO_2 in a tissue culture incubator. BMEOCs were passaged and maintained in endothelial cell growth media (EGM2) using standard techniques. BMEOCs were stained with endothelial cell specific von Wildebrand factor (vWF, DAKO).

Tubular prTE grafts were rehydrated in growth media for 1 hour. Vessels were inoculated with BMEOCs (5×10^3 cells/cm^2) and held at 90 mmHg for 1 hour. Grafts were then maintained in a cell culture incubator for 48 hours in standard conditions. Grafts were fixed with 2.5% paraformaldehyde at 48 hours and evaluated for cell engraftment with DAPI nuclear stain and rhodamine phalloidin f-actin stain. Confocal images were taken with a 63X oil objective on a Zeiss Multiphoton Confocal microscope using 543 and 780 nm excitation wavelengths.

2.8. Statistical analyses

All data are expressed as the mean ± standard deviation. Student's *t*-test, linear regression, and one-way ANOVA with Tukey post hoc tests were used for hypothesis testing, with $p < 0.05$ as the measure for statistical significance. The number of independent tests is listed for each experiment.

3. Results and Discussion

Electrospinning has proven to be a valuable tool to produce biomimetic scaffolds for use in tissue engineering. Electrospun vascular graft materials have included natural proteins, such as collagen and elastin, and biodegradable polymers either as stand alone materials or as blends with other polymers or natural proteins [33, 56, 76]. The number of materials used for electrospinning is increasing as well as the design complexity with multilayered constructs [16, 58, 59, 77, 78] and materials with tunable mechanical properties [59, 78, 79]. Elastin is emerging as an important component of vascular graft development with our increased understanding that synthetic polymers alone pose problems with compliance mismatch and foreign body response [56]. Elastin has unique properties making it a natural choice as a component in vascular scaffold biomaterials that require long-term durability, antithrombogenic properties, and elasticity. Elastin is highly insoluble with a half life of greater than 70 years; it modulates cell function reducing the thrombogenic potential of the surface; and it is highly elastic thus adding compliance to the structure of the biomaterial [80]. Electrospinning of tropoelastin into a biomaterial was first reported in 2005 [51]. Widespread use of tropoelastin for biomaterial development has been limited by the availability of monomeric tropoelastin. Since 2005, the use of tropoelastin has increased and has been incorporated into additional vascular graft scaffolds [78, 80] and coatings on stent struts [81]. The current work describes methods of electrospinning recombinant human tropoelastin into tubular grafts, cross-linking the material into a stable polymer, and characterizing its structural, mechanical, and cell compatibility properties.

3.1. Morphology and Substructure of prTE Fibers

To produce purely electrospun prTE tubular scaffolds, 15 wt% solutions of rTE were electrospun onto rotating mandrels and cross-linked. Conduits were 4-10 cm in length, 4 mm in diameter, with wall thicknesses of 0.43-0.65 mm (Figure 3A). The wall thickness was dependent on the volume of the rTE solution used. The prTE fibers were randomly oriented as determined using image analysis to calculate the probability distribution function of fiber orientation angles relative to horizontal (Figure 4). The average fiber diameters (580 94 nm) and fiber structure (Figure 3B) of the electrospun protein was maintained throughout the thickness of the graft (data not shown).

3.2. Mechanical Properties of prTE

Uni-axial tensile testing of prTE samples from 15 wt% rTE produced stress-strain curves (Figure 5) for both the longitudinal and circumferential sample orientations. The curves were similar for the two orientations showing a bimodal stress-strain relationship in which the modulus was dependent on the percent strain. The transition in moduli values occurred

between 40 and 50% strain. The only mechanical property that was significantly different between the longitudinal and circumferential orientations of electrospun prTE was the elastic modulus 2 (t-test, $p < 0.01$). The remaining mechanical properties (UTS, % elongation, and elastic modulus 1) were not significantly different (t-test, $p > 0.05$) between the two orientations (Figure 6). Combining electrospun prTE's longitudinal and circumferential orientations measurements, the average UTS, elastic modulus 1 and percent elongation were 0.36 ± 0.05 MPa, 0.15 ± 0.04 MPa, and 77 ± 5%, respectively. Elastic modulus 2 values were not combined because they were significantly different between orientations.

Ultimate tensile strength (UTS), percent elongation, and elastic moduli for electrospun prTE were compared to extracted porcine elastin and native porcine carotid arteries for the longitudinal (L) and circumferential (C) orientations (Figure 6). The electrospun prTE samples had UTS values of 0.34 ± 0.14 MPa (C) and 0.38 ± 0.05 MPa (L). The UTS values for the electrospun prTE were comparable to extracted porcine elastin in the longitudinal direction, yet significantly different to circumferential extracted elastin and both native carotid artery specimens (ANOVA, Tukey post hoc, $p < 0.05$). The percent elongation at failure of the electrospun prTE was 79 ± 6% (C) and 75 ± 5% (L), which was significantly lower than the control materials in both orientations (ANOVA, Tukey post hoc, $p < 0.01$). The average elastic moduli of electrospun prTE were 0.15 ± 0.05 MPa (C) and 0.15 ± 0.03 MPa (L) for elastic modulus 1 and 0.82 ± 0.11 MPa, (C) and 0.99 ± 0.17 MPa (L) for elastic modulus 2 which were comparable to extracted elastin in the longitudinal direction for elastic modulus 1 and in both orientations for elastic modulus 2. Both prTE elastic moduli were significantly different from the native carotid materials (ANOVA, Tukey post hoc, $p < 0.05$)

Average compliance values for electrospun prTE, extracted elastin, and native carotid arteries were 20.2 2.6, 32.0 3.1 and 3.4 0.5 % respectively, which were all significantly different (ANOVA, Tukey post hoc, $p < 0.01$). Extracted elastin lacks collagen and therefore is expected to have greater compliance. The compliance of electrospun prTE fell between extracted elastin and native carotid arteries. This allows for the addition of stiffer materials, such as collagen, to the biomaterial to both strengthen the vessel in terms of UTS while maintaining compliance equivalent to native vessels.

The mechanical properties of electrospun proteins are dependent on the specific proteins selected, the protein concentration, electrospinning parameters, cross-linkers, and fiber orientation [51, 76, 85-87]. The mechanical properties of the circumferential and longitudinal orientations of the prTE materials were similar, where the only measured significant difference was in the elastic modulus 2 of electrospun prTE. UTS values of prTE electrospun materials were between the values of native extracted elastin in the longitudinal and circumferential directions and were much lower than the native carotid artery [88-93]. These results were expected due to the random (non-oriented) nature of the electrospun prTE fibers compared with the oriented fibers of native elastin [94], and due to the presence of collagen in the native matrix. Additionally, the elastic modulus 1 of electrospun prTE, measured on the initial linear slope of the stress-strain curve, were comparable to the extracted elastin. Native elastic fibers (composed of elastin and fibrillin-1) contribute significantly to the material properties of native elastic arteries [95] in this initial linear slope region of the stress-strain curve. Native arteries are true composites of matrix proteins and the transition in elastic modulus is primarily due to elastin and collagen's unique mechanical contributions working in concert. Therefore, the incorporation of prTE into a collagen scaffold is likely to increase the compliance of the vascular graft. The material properties of the electrospun prTE biomaterials were significantly different from the electrospun human tropoelastin by Li et al. [51]. The prTE had lower average UTS (0.36 MPa vs. 13 MPa) and

average elastic moduli (0.15 MPa (elastic modulus 1) and 0.91 MPa (elastic modulus 2) vs. 289 MPa), yet a higher average percent elongation at failure (77% vs. 15%). It should be noted that only a single mechanical test was reported for Li's electrospun tropoelastin due to limited availability of protein [51]. The prTE materials were more elastic with a lower failure stress than Li's previously reported electrospun tropoelastin [51]. These disparities could be due to significant differences in electrospinning methods, testing methods, and cross-linking strategies. Our electrospinning parameters differ from Li et al., in several ways, including lower concentration of tropoelastin, higher accelerating voltage, and a smaller gap distance, which resulted in smaller and cylindrically-shaped fibers [96] for our prTE. The mechanical property evaluation by Li et al. utilized a unique testing system designed to evaluate textiles, which included the measured material weight to calculate stress. This measurement can be variable due to differences in the hydration of the tropoelastin. Our engineering stress calculations were based on the measured initial cross-sectional area. Additionally, to crosslink the tropoelastin Li et al. used hexamethylene diisocyanate (HMDI), which binds lysine or hydroxylysine residues, but may also react with nucleophilic functional groups such as amines, alcohols, and protonated acids. HMDI has been shown to react with side chains of lysine, cysteine, histidine and tyrosine and may as well react to arginine, and aspartic acid. Nonspecific binding of residues by HMDI may affect the functionality and water content [97], thus altering the mechanical properties of cross-linked tropoelastin. DSS in comparison is specific to amines on lysine residues with an 8 atom bridge resulting in a 11.4 Angstrom crosslink arm. The specificity of DSS to lysine [98] leaves the cell binding domains available on the molecule as well as results in improved consistency of mechanical properties.

The mechanical properties were comparable to extracted elastin scaffolds, but still lack the tensile strength to support *in vivo* arterial pressures. For vascular graft applications, the tensile strengths of the prTE scaffolds must be further increased by reinforcement or co-spinning with either collagen or synthetic materials.

3.3. Burst Pressure of prTE Scaffolds

The electrospun prTE tubular scaffolds (n=3) had an average wall thickness of 453 74 μm and an average burst pressure of 485 25 mmHg. Scaffolds increased in size both longitudinally and circumferentially throughout the burst pressure test and test samples failed longitudinally in all cases. Saphenous vein and internal mammary artery grafts, the gold standard treatments, have reported burst pressures of 1599 877 and 3196 1264 mmHg, respectively [101]. Extracted porcine carotid elastin has a reported burst pressure of 162 ± 36 mmHg [69], which is significantly lower than the electrospun prTE, however, the UTS measurements were comparable between our electrospun and extracted elastin samples. Burst pressure differences could be due simply to differences in wall thickness or a more complex mechanism involving variations in fiber architecture, which would lead to altered loading on individual fibers during biaxial deformation of the matrix. While an average burst pressure of 485 mmHg for our electrospun graft is sufficient for initial *in vivo* testing of host response, higher failure pressures of at least 1500 mmHg would need to be achieved to give an ample safety factor (>10) for its widespread clinical use.

3.4. Endothelial Cell Growth on prTE Scaffolds

Organic solvents, such as HFP, facilitate the electrospinning of pure protein solutions, due to improved protein solubility and solvent volatility. HFP has been shown to affect the conformation of electrospun collagen [99], which could have a drastic effect on its stability and mechanical properties. Tropoelastin is unlikely to be affected, as it is a single chain molecule that easily regains its secondary structure on removal of denaturants. The similarity in mechanical properties of prTE and extracted native elastin indicate minimal

conformational changes in the prTE. The cytotoxic effects of HFP must be considered in construct design. HFP at concentrations above 250 ppm is toxic to cells [100]. The residual solvent HFP can be present in electrospun materials, but is likely removed through post processing (heat/vacuum treatments) of the material [100]. Our electrospun materials have been shown to support vascular cell growth [96], thus indicating low residual solvent levels, but a full evaluation of residual HFP should be conducted prior to conducting *in vivo* implant studies.

Bone marrow derived endothelial outgrowth cells (BMEOCs) attached, spread, and grew on the 15 wt% prTE tubular scaffolds. BMEOCs stained positive for vWF indicating an endothelial cell population (Figure 7A & B). Confocal images taken at 48 hours showed cells well attached and spread on the electrospun fiber matrix. Cells formed a confluent monolayer with typical endothelial cell cobblestone morphology (Figure 7C). This supports the hypothesis that prTE is a cell compatible matrix for both endothelial cells as well as, previously reported, smooth muscle cells [102], which demonstrated positive SMC growth and proliferation on prTE over a week with logarithmic cell growth between 3 and 5 days via integrin mediated binding mechanisms.

4. Conclusions

An electrospun tubular vascular scaffold material has been developed, composed of cross-linked recombinant human tropoelastin, which has physical and mechanical properties similar to extracted arterial elastin. The graft architecture, i.e. length and diameter, of the prTE scaffold can be precisely designed and controlled. A cross-linked stable polymer assembled from recombinant human tropoelastin provides both the compliance and support of endothelial cell adhesion for a component of a vascular graft biomaterial. While the mechanical strength of the prTE scaffolds are insufficient for implantation alone, the relatively lower compliance compared to native arteries will allow for the addition of stronger, but stiffer biomaterials. This technology holds great promise for incorporation in small diameter vascular graft biomaterials.

Acknowledgments

We would like to thank Dr. Michael Rutten for isolation of the bone marrow mononuclear cells and Dr. Sean Kirkpatrick for assistance with fiber orientation code development. Tropoelastin was produced with the excellent technical assistance of Amy Jay, Cher Hawkey, and Rose Merten. This work was funded in part by the NIH R01-HL095474, NIH R01-HL103728, and the Department of the Army, Grant Nos. W81XWH-04-1-0841 and W81XWH-05-1-0586. This work does not necessarily reflect the policy of the government and no official endorsement should be inferred.

References

[1]. Lloyd-Jones D, Adams RJ, Brown TM, Carnethon M, Dai S, De Simone G, et al. Heart disease and stroke statistics--2010 update: a report from the American Heart Association. Circulation. 2010; 121:e46–e215. [PubMed: 20019324]

[2]. Brewster, D. Prosthetic Grafts. In: Rutherford, Rd, editor. Vascular Surgery. 1995. p. 492-508.

[3]. Abbott, WM.; Rehring, TF. Biologic and synthetic prosthetic materials for vascular conduits. In: Hobson, RW.; Wilson, S.; Veith, FJ., editors. Vascular Surgery: Principles and Practice. 3rd Edition. Marcel Dekker; New York: 2004. p. 611-20.

[4]. McGuigan AP, Sefton MV. The influence of biomaterials on endothelial cell thrombogenicity. Biomaterials. 2007; 28:2547–71. [PubMed: 17316788]

[5]. Sarkar S, Sales KM, Hamilton G, Seifalian AM. Addressing thrombogenicity in vascular graft construction. J Biomed Mater Res B Appl Biomater. 2007; 82:100–8. [PubMed: 17078085]

[6]. Sawyer PN, Fitzgerald J, Kaplitt MJ, Sanders RJ, Williams GM, Leather RP, et al. Ten year experience with the negatively charged glutaraldehyde-tanned vascular graft in peripheral vascular surgery. Initial multicenter trial. Am J Surg. 1987; 154:533–7. [PubMed: 3314542]

[7]. Dardik H, Wengerter K, Qin F, Pangilinan A, Silvestri F, Wolodiger F, et al. Comparative decades of experience with glutaraldehyde-tanned human umbilical cord vein graft for lower limb revascularization: an analysis of 1275 cases. J Vasc Surg. 2002; 35:64–71. [PubMed: 11802134]

[8]. Strobel R, Boontje AH, Van Den Dungen JJ. Aneurysm formation in modified human umbilical vein grafts. Eur J Vasc Endovasc Surg. 1996; 11:417–20. [PubMed: 8846174]

[9]. Gui L, Muto A, Chan SA, Breuer CK, Niklason LE. Development of decellularized human umbilical arteries as small-diameter vascular grafts. Tissue Eng Part A. 2009; 15:2665–76. [PubMed: 19207043]

[10]. Brennan MP, Dardik A, Hibino N, Roh JD, Nelson GN, Papademitris X, et al. Tissue-engineered vascular grafts demonstrate evidence of growth and development when implanted in a juvenile animal model. Ann Surg. 2008; 248:370–7. [PubMed: 18791357]

[11]. Campbell JH, Efendy JL, Campbell GR. Novel vascular graft grown within recipient's own peritoneal cavity. Circ Res. 1999; 85:1173–8. [PubMed: 10590244]

[12]. L'Heureux N, Dusserre N, Marini A, Garrido S, de la Fuente L, McAllister T. Technology insight: the evolution of tissue-engineered vascular grafts--from research to clinical practice. Nature clinical practice. 2007; 4:389–95.

[13]. McAllister TN, Maruszewski M, Garrido SA, Wystrychowski W, Dusserre N, Marini A, et al. Effectiveness of haemodialysis access with an autologous tissue-engineered vascular graft: a multicentre cohort study. Lancet. 2009; 373:1440–6. [PubMed: 19394535]

[14]. Roh JD, Sawh-Martinez R, Brennan MP, Jay SM, Devine L, Rao DA, et al. Tissue-engineered vascular grafts transform into mature blood vessels via an inflammation-mediated process of vascular remodeling. Proc Natl Acad Sci U S A. 2010; 107:4669–74. [PubMed: 20207947]

[15]. Shin'oka T, Matsumura G, Hibino N, Naito Y, Watanabe M, Konuma T, et al. Midterm clinical result of tissue-engineered vascular autografts seeded with autologous bone marrow cells. J Thorac Cardiovasc Surg. 2005; 129:1330–8. [PubMed: 15942574]

[16]. Cao Y, Zhang B, Croll T, Rolfe BE, Campbell JH, Campbell GR, et al. Engineering tissue tubes using novel multilayered scaffolds in the rat peritoneal cavity. J Biomed Mater Res A. 2008; 87:719–27. [PubMed: 18200539]

[17]. Stickler P, De Visscher G, Mesure L, Famaey N, Martin D, Campbell JH, et al. Cyclically stretching developing tissue in vivo enhances mechanical strength and organization of vascular grafts. Acta Biomater. 2010; 6:2448–56. [PubMed: 20123137]

[18]. Steinhoff G, Stock U, Karim N, Mertsching H, Timke A, Meliss RR, Pethig K, Haverich A, Bader A. Tissue engineering of pulmonary heart valves on allogenic acellular matrix conduits: in vivo restoration of valve tissue. Circulation. 2000; 102(19 Suppl 3):III50–5. [PubMed: 11082362]

[19]. Courtman DW, Errett BF, Wilson GJ. The role of crosslinking in modification of the immune response elicited against xenogenic vascular acellular matrices. J Biomed Mater Res. 2001; 55(4):576–86. [PubMed: 11288086]

[20]. Abbott WM, Megerman J, Hasson JE, L'Italien G, Warnock DF. Effect of compliance mismatch on vascular graft patency. J Vasc Surg. 1987; 5:376–82. [PubMed: 3102762]

[21]. Baird RN, Abbott WM. Pulsatile blood-flow in arterial grafts. Lancet. 1976; 2:948–50. [PubMed: 62175]

[22]. Kidson IG, Abbott WM. Low compliance and arterial graft occlusion. Circulation. 1978; 58:I1–4. [PubMed: 14740668]

[23]. Hunter GC, Carson SN, Wong HN, French S. Experimental small-diameter graft patency: effect of compliance, porosity and graft healing potential. Curr Surg. 1980; 37:439–41. [PubMed: 7214995]

[24]. Kidson IG. The effect of wall mechanical properties on patency of arterial grafts. Ann R Coll Surg Engl. 1983; 65:24–9. [PubMed: 6218775]

[25]. Clark RE, Apostolou S, Kardos JL. Mismatch of mechanical properties as a cause of arterial prostheses thrombosis. Surg Forum. 1976; 27:208–10. [PubMed: 1019858]

[26]. Kinley CE, Marble AE. Compliance: a continuing problem with vascular grafts. J Cardiovasc Surg (Torino). 1980; 21:163–70.

[27]. Okuhn SP, Connelly DP, Calakos N, Ferrell L, Pan MX, Goldstone J. Does compliance mismatch alone cause neointimal hyperplasia? J Vasc Surg. 1989; 9:35–45. [PubMed: 2911141]

[28]. Uchida N, Kambic H, Emoto H, Chen JF, Hsu S, Murabayshi S, et al. Compliance effects on small diameter polyurethane graft patency. Journal of biomedical materials research. 1993; 27:1269–79. [PubMed: 8245041]

[29]. Wu MH, Shi Q, Sauvage LR, Kaplan S, Hayashida N, Patel MD, et al. The direct effect of graft compliance mismatch per se on development of host arterial intimal hyperplasia at the anastomotic interface. Ann Vasc Surg. 1993; 7:156–68. [PubMed: 8518133]

[30]. Murugan R, Ramakrishna S. Nano-featured scaffolds for tissue engineering: a review of spinning methodologies. Tissue engineering. 2006; 12:435–47. [PubMed: 16579677]

[31]. Zhang X, Thomas V, Xu Y, Bellis SL, Vohra YK. An in vitro regenerated functional human endothelium on a nanofibrous electrospun scaffold. Biomaterials. 2010; 31:4376–81. [PubMed: 20199808]

[32]. Zhang X, Thomas V, Vohra YK. Two ply tubular scaffolds comprised of proteins/poliglecaprone/polycaprolactone fibers. J Mater Sci Mater Med. 2010; 21:541–9. [PubMed: 19902335]

[33]. McClure MJ, Sell SA, Simpson DG, Walpoth BH, Bowlin GL. A three-layered electrospun matrix to mimic native arterial architecture using polycaprolactone, elastin, and collagen: A preliminary study. Acta Biomater. 2010

[34]. Pham QP, Sharma U, Mikos AG. Electrospinning of polymeric nanofibers for tissue engineering applications: a review. Tissue Eng. 2006; 12:1197–211. [PubMed: 16771634]

[35]. Bhattarai SR, Bhattarai N, Yi HK, Hwang PH, Cha DI, Kim HY. Novel biodegradable electrospun membrane: scaffold for tissue engineering. Biomaterials. 2004; 25:2595–602. [PubMed: 14751745]

[36]. Katti DS, Robinson KW, Ko FK, Laurencin CT. Bioresorbable nanofiber-based systems for wound healing and drug delivery: optimization of fabrication parameters. J Biomed Mater Res B Appl Biomater. 2004; 70:286–96. [PubMed: 15264311]

[37]. Kim K, Yu M, Zong X, Chiu J, Fang D, Seo YS, et al. Control of degradation rate and hydrophilicity in electrospun non-woven poly(D,L-lactide) nanofiber scaffolds for biomedical applications. Biomaterials. 2003; 24:4977–85. [PubMed: 14559011]

[38]. Li WJ, Laurencin CT, Caterson EJ, Tuan RS, Ko FK. Electrospun nanofibrous structure: a novel scaffold for tissue engineering. Journal of biomedical materials research. 2002; 60:613–21. [PubMed: 11948520]

[39]. Khil MS, Cha DI, Kim HY, Kim IS, Bhattarai N. Electrospun nanofibrous polyurethane membrane as wound dressing. J Biomed Mater Res B Appl Biomater. 2003; 67:675–9. [PubMed: 14598393]

[40]. Li WJ, Danielson KG, Alexander PG, Tuan RS. Biological response of chondrocytes cultured in three-dimensional nanofibrous poly(epsilon-caprolactone) scaffolds. J Biomed Mater Res A. 2003; 67:1105–14. [PubMed: 14624495]

[41]. Mo XM, Xu CY, Kotaki M, Ramakrishna S. Electrospun P(LLA-CL) nanofiber: a biomimetic extracellular matrix for smooth muscle cell and endothelial cell proliferation. Biomaterials. 2004; 25:1883–90. [PubMed: 14738852]

[42]. Shin M, Ishii O, Sueda T, Vacanti JP. Contractile cardiac grafts using a novel nanofibrous mesh. Biomaterials. 2004; 25:3717–23. [PubMed: 15020147]

[43]. Shin M, Yoshimoto H, Vacanti JP. In vivo bone tissue engineering using mesenchymal stem cells on a novel electrospun nanofibrous scaffold. Tissue engineering. 2004; 10:33–41. [PubMed: 15009928]

[44]. Xu CY, Inai R, Kotaki M, Ramakrishna S. Aligned biodegradable nanofibrous structure: a potential scaffold for blood vessel engineering. Biomaterials. 2004; 25:877–86. [PubMed: 14609676]

[45]. Yoshimoto H, Shin YM, Terai H, Vacanti JP. A biodegradable nanofiber scaffold by electrospinning and its potential for bone tissue engineering. Biomaterials. 2003; 24:2077–82. [PubMed: 12628828]

[46]. Boland ED, Matthews JA, Pawlowski KJ, Simpson DG, Wnek GE, Bowlin GL. Electrospinning collagen and elastin: preliminary vascular tissue engineering. Front Biosci. 2004; 9:1422–32. [PubMed: 14977557]

[47]. Buttafoco L, Kolkman NG, Engbers-Buijtenhuijs P, Poot AA, Dijkstra PJ, Vermes I, et al. Electrospinning of collagen and elastin for tissue engineering applications. Biomaterials. 2006; 27:724–34. [PubMed: 16111744]

[48]. Buttafoco L, Kolkman NG, Poot AA, Dijkstra PJ, Vermes I, Feijen J. Electrospinning collagen and elastin for tissue engineering small diameter blood vessels. J Control Release. 2005; 101:322–4. [PubMed: 15719516]

[49]. Lee SJ, Yoo JJ, Lim GJ, Atala A, Stitzel J. In vitro evaluation of electrospun nanofiber scaffolds for vascular graft application. J Biomed Mater Res A. 2007; 83:999–1008. [PubMed: 17584890]

[50]. Li M, Mondrinos MJ, Chen X, Gandhi MR, Ko FK, Lelkes PI. Co-electrospun poly(lactide-co-glycolide), gelatin, and elastin blends for tissue engineering scaffolds. J Biomed Mater Res A. 2006; 79:963–73. [PubMed: 16948146]

[51]. Li M, Mondrinos MJ, Gandhi MR, Ko FK, Weiss AS, Lelkes PI. Electrospun protein fibers as matrices for tissue engineering. Biomaterials. 2005; 26:5999–6008. [PubMed: 15894371]

[52]. Stitzel J, Liu J, Lee SJ, Komura M, Berry J, Soker S, et al. Controlled fabrication of a biological vascular substitute. Biomaterials. 2006; 27:1088–94. [PubMed: 16131465]

[53]. El-Kurdi MS, Hong Y, Stankus JJ, Soletti L, Wagner WR, Vorp DA. Transient elastic support for vein grafts using a constricting microfibrillar polymer wrap. Biomaterials. 2008; 29:3213–20. [PubMed: 18455787]

[54]. Abbott, WM.; Rehring, TF. Biologic and Synthetic Prosthetic Materials for Vascular Conduits. In: Hobson, RW.; WIlson, SE.; Veith, FJ., editors. Vascular Surgery: Principles and Practice. 3rd ed.. Marcel Dekker; New York: 2004. p. 611-20.

[55]. Annabi N, Mithieux SM, Boughton EA, Ruys AJ, Weiss AS, Dehghani F. Synthesis of highly porous crosslinked elastin hydrogels and their interaction with fibroblasts in vitro. Biomaterials. 2009; 30:4550–7. [PubMed: 19500832]

[56]. Smith MJ, McClure MJ, Sell SA, Barnes CP, Walpoth BH, Simpson DG, et al. Suture-reinforced electrospun polydioxanone-elastin small-diameter tubes for use in vascular tissue engineering: a feasibility study. Acta Biomater. 2008; 4:58–66. [PubMed: 17897890]

[57]. Sallach RE, Cui W, Wen J, Martinez A, Conticello VP, Chaikof EL. Elastin-mimetic protein polymers capable of physical and chemical crosslinking. Biomaterials. 2009; 30:409–22. [PubMed: 18954902]

[58]. Caves JM, Cui W, Wen J, Kumar VA, Haller CA, Chaikof EL. Elastin-like protein matrix reinforced with collagen microfibers for soft tissue repair. Biomaterials. 2011; 32:5371–9. [PubMed: 21550111]

[59]. Caves JM, Kumar VA, Martinez AW, Kim J, Ripberger CM, Haller CA, et al. The use of microfiber composites of elastin-like protein matrix reinforced with synthetic collagen in the design of vascular grafts. Biomaterials. 2010; 31:7175–82. [PubMed: 20584549]

[60]. Roach MR, Burton AC. The reason for the shape of the distensibility curves of arteries. Canadian journal of biochemistry and physiology. 1957; 35:681–90. [PubMed: 13460788]

[61]. Baxter BT, McGee GS, Shively VP, Drummond IA, Dixit SN, Yamauchi M, et al. Elastin content, cross-links, and mRNA in normal and aneurysmal human aorta. J Vasc Surg. 1992; 16:192–200. [PubMed: 1495142]

[62]. Curran ME, Atkinson DL, Ewart AK, Morris CA, Leppert MF, Keating MT. The elastin gene is disrupted by a translocation associated with supravalvular aortic stenosis. Cell. 1993; 73:159–68. [PubMed: 8096434]

[63]. Ewart AK, Jin W, Atkinson D, Morris CA, Keating MT. Supravalvular aortic stenosis associated with a deletion disrupting the elastin gene. The Journal of clinical investigation. 1994; 93:1071–7. [PubMed: 8132745]

[64]. Gandhi RH, Irizarry E, Cantor JO, Keller S, Nackman GB, Halpern VJ, et al. Analysis of elastin cross-linking and the connective tissue matrix of abdominal aortic aneurysms. Surgery. 1994; 115:617–20. [PubMed: 8178261]

[65]. Hunter GC, Dubick MA, Keen CL, Eskelson CD. Effects of hypertension on aortic antioxidant status in human abdominal aneurysmal and occlusive disease. Proc Soc Exp Biol Med. 1991; 196:273–9. [PubMed: 1998004]

[66]. Li DY, Toland AE, Boak BB, Atkinson DL, Ensing GJ, Morris CA, et al. Elastin point mutations cause an obstructive vascular disease, supravalvular aortic stenosis. Human molecular genetics. 1997; 6:1021–8. [PubMed: 9215670]

[67]. Rizzo RJ, McCarthy WJ, Dixit SN, Lilly MP, Shively VP, Flinn WR, et al. Collagen types and matrix protein content in human abdominal aortic aneurysms. J Vasc Surg. 1989; 10:365–73. [PubMed: 2795760]

[68]. Urban Z, Michels VV, Thibodeau SN, Donis-Keller H, Csiszar K, Boyd CD. Supravalvular aortic stenosis: a splice site mutation within the elastin gene results in reduced expression of two aberrantly spliced transcripts. Human genetics. 1999; 104:135–42. [PubMed: 10190324]

[69]. Hinds MT, Rowe RC, Ren Z, Teach J, Wu PC, Kirkpatrick SJ, et al. Development of a reinforced porcine elastin composite vascular scaffold. J Biomed Mater Res A. 2006; 77:458–69. [PubMed: 16453334]

[70]. Karnik SK, Brooke BS, Bayes-Genis A, Sorensen L, Wythe JD, Schwartz RS, et al. A critical role for elastin signaling in vascular morphogenesis and disease. Development (Cambridge, England). 2003; 130:411–23.

[71]. Daamen WF, Veerkamp JH, van Hest JC, van Kuppevelt TH. Elastin as a biomaterial for tissue engineering. Biomaterials. 2007; 28:4378–98. [PubMed: 17631957]

[72]. Patel A, Fine B, Sandig M, Mequanint K. Elastin biosynthesis: The missing link in tissue-engineered blood vessels. Cardiovasc Res. 2006; 71:40–9. [PubMed: 16566911]

[73]. ANSI. AAMI. ISO. Cardiovascular implants—Tubular vascular prostheses. 2001. 7198:1998/2001

[74]. Rutten M, Janes MA, Laraway B, Gregory C, Gregory K. Comparison of quantum dots and CM-DiI for labeling porcine autologous bone marrow mononuclear cells. The Open Stem Cell Journal. 2010; 2:25–36.

[75]. Barnes CP, Sell SA, Boland ED, Simpson DG, Bowlin GL. Nanofiber technology: designing the next generation of tissue engineering scaffolds. Adv Drug Deliv Rev. 2007; 59:1413–33. [PubMed: 17916396]

[76]. Sell SA, McClure MJ, Barnes CP, Knapp DC, Walpoth BH, Simpson DG, et al. Electrospun polydioxanone-elastin blends: potential for bioresorbable vascular grafts. Biomed Mater. 2006; 1:72–80. [PubMed: 18460759]

[77]. Huang C, Chen R, Ke Q, Morsi Y, Zhang K, Mo X. Electrospun collagen-chitosan-TPU nanofibrous scaffolds for tissue engineered tubular grafts. Colloids Surf B Biointerfaces. 2011; 82:307–15. [PubMed: 20888196]

[78]. Wise SG, Byrom MJ, Waterhouse A, Bannon PG, Weiss AS, Ng MK. A multilayered synthetic human elastin/polycaprolactone hybrid vascular graft with tailored mechanical properties. Acta Biomater. 2011; 7:295–303. [PubMed: 20656079]

[79]. Bonani W, Maniglio D, Motta A, Tan W, Migliaresi C. Biohybrid nanofiber constructs with anisotropic biomechanical properties. J Biomed Mater Res B Appl Biomater. 2011; 96:276–86. [PubMed: 21210507]

[80]. Wise SG, Mithieux SM, Weiss AS. Engineered tropoelastin and elastin-based biomaterials. Adv Protein Chem Struct Biol. 2009; 78:1–24. [PubMed: 20663482]

[81]. Waterhouse A, Yin Y, Wise SG, Bax DV, McKenzie DR, Bilek MM, et al. The immobilization of recombinant human tropoelastin on metals using a plasma-activated coating to improve the biocompatibility of coronary stents. Biomaterials. 2010; 31:8332–40. [PubMed: 20708259]

[82]. Faury G, Pezet M, Knutsen RH, Boyle WA, Heximer SP, McLean SE, et al. Developmental adaptation of the mouse cardiovascular system to elastin haploinsufficiency. J Clin Invest. 2003; 112:1419–28. [PubMed: 14597767]

[83]. Li DY, Brooke B, Davis EC, Mecham RP, Sorensen LK, Boak BB, et al. Elastin is an essential determinant of arterial morphogenesis. Nature. 1998; 393:276–80. [PubMed: 9607766]

[84]. Li DY, Faury G, Taylor DG, Davis EC, Boyle WA, Mecham RP, et al. Novel arterial pathology in mice and humans hemizygous for elastin. J Clin Invest. 1998; 102:1783–7. [PubMed: 9819363]

[85]. Huang L, Nagapudi K, Apkarian RP, Chaikof EL. Engineered collagen-PEO nanofibers and fabrics. Journal of biomaterials science. 2001; 12:979–93.

[86]. Matthews JA, Wnek GE, Simpson DG, Bowlin GL. Electrospinning of collagen nanofibers. Biomacromolecules. 2002; 3:232–8. [PubMed: 11888306]

[87]. Zeugolis DI, Paul GR, Attenburrow G. Cross-linking of extruded collagen fibers-A biomimetic three-dimensional scaffold for tissue engineering applications. J Biomed Mater Res A. 2008

[88]. Cohen J, Litwin SB, Aaron A, Fine S. The rupture force and tensile strength of canine aortic tissue. The Journal of surgical research. 1972; 13:321–33. [PubMed: 4652936]

[89]. Coulson WF. The effect of proteolytic enzymes on the tensile strength of whole aorta and isolated aortic elastin. Biochimica et biophysica acta. 1971; 237:378–86. [PubMed: 4105895]

[90]. Haut RC, Garg BD, Metke M, Josa M, Kaye MP. Mechanical properties of the canine aorta following hypercholesterolemia. Journal of biomechanical engineering. 1980; 102:98–102. [PubMed: 6968001]

[91]. Hayashi K. Fundamental and applied studies of mechanical properties of cardiovascular tissues. Biorheology. 1982; 19:425–36. [PubMed: 7049265]

[92]. Litwin SB, Cohen J, Fine S. Effects of sterilization and preservation on the rupture force and tensile strength of canine aortic tissue. The Journal of surgical research. 1973; 15:198–206. [PubMed: 4728349]

[93]. Purslow PP. Positional variations in fracture toughness, stiffness and strength of descending thoracic pig aorta. Journal of biomechanics. 1983; 16:947–53. [PubMed: 6654923]

[94]. Farand P, Garon A, Plante GE. Structure of large arteries: Orientation of elastin in rabbit aortic internal elastic lamina and in the elastic lamellae of aortic media. Microvascular Research. 2007; 73:95–9. [PubMed: 17174983]

[95]. Carta L, Wagenseil JE, Knutsen RH, Mariko B, Faury G, Davis EC, et al. Discrete contributions of elastic fiber components to arterial development and mechanical compliance. Arterioscler Thromb Vasc Biol. 2009; 29:2083–9. [PubMed: 19850904]

[96]. McKenna KA, Gregory KW, Sarao RC, Maslen CL, Glanville RW, Hinds MT. Structural and cellular characterization of electrospun recombinant human tropoelastin biomaterials. J Biomater Appl. 2011

[97]. Nowatzki PJ, Tirrell DA. Physical properties of artificial extracellular matrix protein films prepared by isocyanate crosslinking. Biomaterials. 2004; 25:1261–7. [PubMed: 14643600]

[98]. Di Zio K, Tirrell DA. Mechanical Properties of Artificial Protein Matrices Engineered for Control of Cell and Tissue Behavior. Macromolecules. 2003; 36:1553–8.

[99]. Zeugolis DI, Khew ST, Yew ES, Ekaputra AK, Tong YW, Yung LY, et al. Electrospinning of pure collagen nano-fibres - just an expensive way to make gelatin? Biomaterials. 2008; 29:2293–305. [PubMed: 18313748]

[100]. Nam J, Huang Y, Agarwal S, Lannutti J. Materials selection and residual solvent retention in biodegradable electrospun fibers. Journal of Applied Polymer Science. 2008; 107:1547–54.

[101]. Konig G, McAllister TN, Dusserre N, Garrido SA, Iyican C, Marini A, et al. Mechanical properties of completely autologous human tissue engineered blood vessels compared to human saphenous vein and mammary artery. Biomaterials. 2009; 30:1542–50. [PubMed: 19111338]

[102]. McKenna KA, Gregory KW, Sarao RC, Maslen CL, Glanville RW, Hinds MT. Structural and cellular characterization of electrospun recombinant human tropoelastin biomaterials. Journal of Biomaterials Applications. 2011 in press.

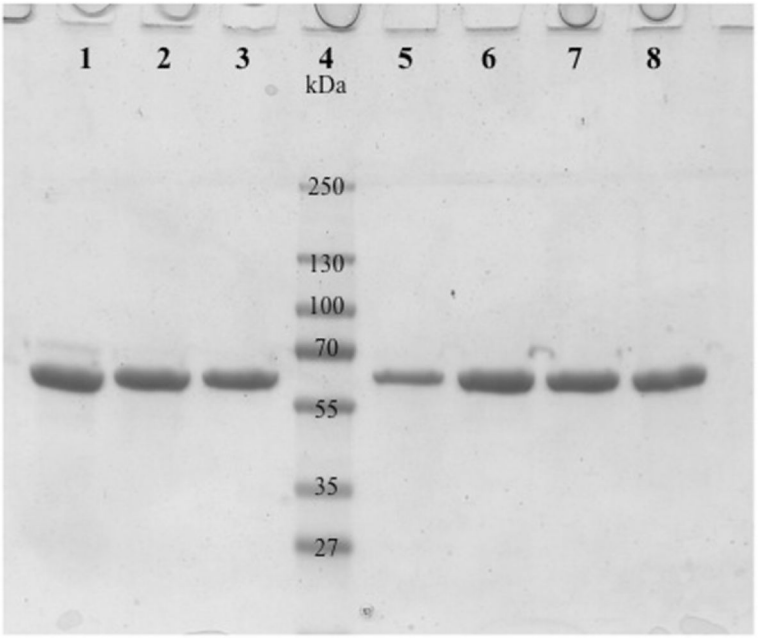

Figure 1.
Stained electrophoresis gel showing purified human tropoelastin from 7 different batches (lanes 1-3 and 5-8) illustrating the purity of the product and reproducibility of the purification process. Lane 4 is a molecular weight standard.

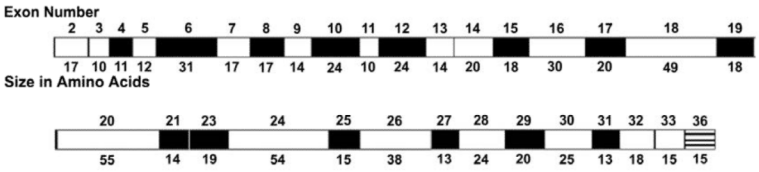

Figure 2.

Diagramatic representation of human tropoelastin protein domains. The number of the corresponding exons and the sizes of the domains are shown. The exon numbering system is based upon the bovine elastin gene sequence. The human gene has no exons 34 and 35, while exon 26A is rarely expressed in human tropoelastin. Cross-linking domains are shaded black and hydrophobic domains are white.

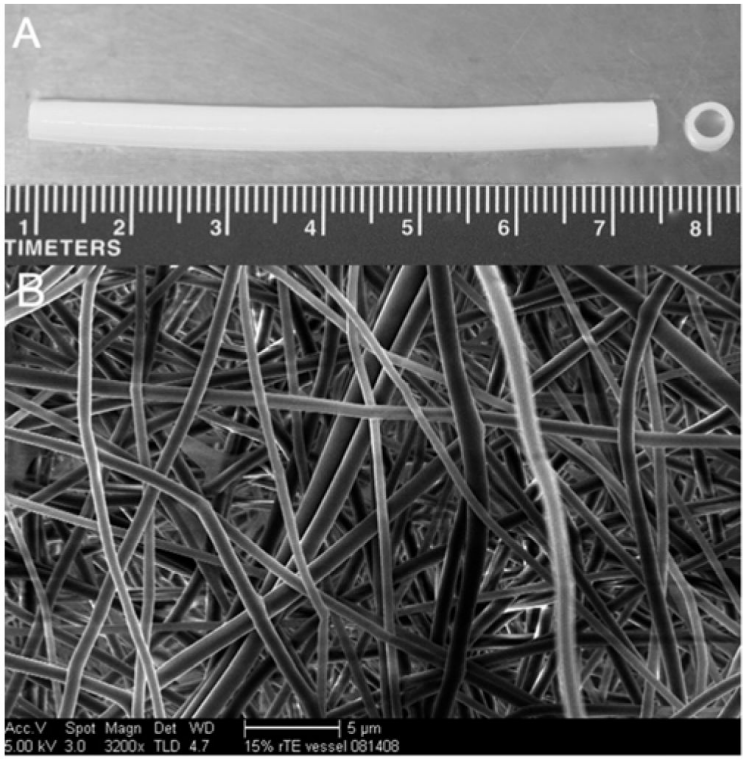

Figure 3.

Electrospun tubular prTE vascular scaffold. **(A)** The vascular scaffold was 7 cm in length, 4 mm internal diameter, and consisted of pure prTE fibers. **(B)** The prTE fibers were randomly oriented with average fiber diameters of 580 94 nm. The scale bar indicates 5 μm.

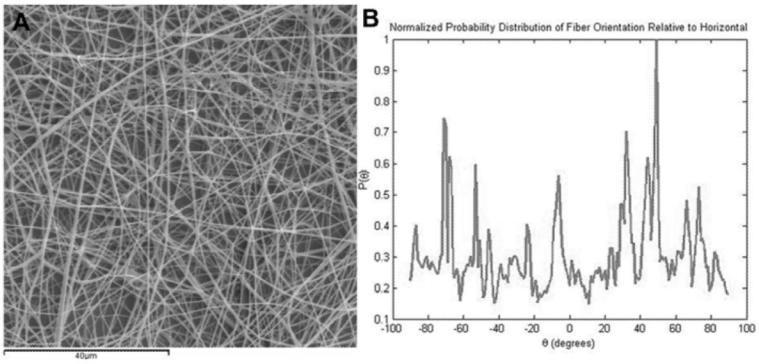

Figure 4.
MATLAB image analysis of fiber orientation. **(A)** Image of electrospun prTE fibers **(B)** Normalized probability distribution function plotted as probability of the feature orientation versus angle. Fibers were randomly oriented in these samples.

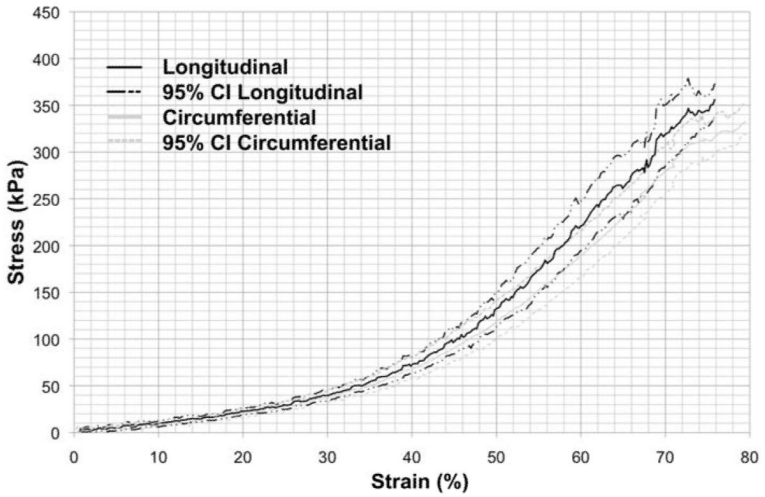

Figure 5.

Average stress-strain curves for electrospun prTE fibers from a 15 wt% solution for both circumferential and longitudinal orientations (average with 95% confidence interval). The only significant difference in mechanical properties was in the elastic modulus 2 of the tested orientations.

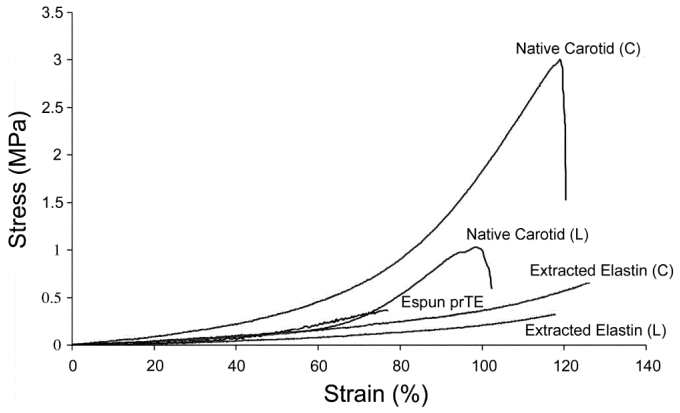

Specimen	UTS (MPa)	Percent Elongation (%)	Elastic Modulus 1 (MPa)	Elastic Modulus 2 (MPa)
Espun prTE (L)	0.38 ± 0.05	75 ± 5	0.15 ± 0.03	0.99 ± 0.17**
Espun prTE (C)	0.34 ± 0.14	79 ± 6	0.15 ± 0.05	0.82 ± 0. 11**
Extracted Elastin (L)	0.29 ± 0.06[a]	107 ± 14*	0.16 ± 0.05[a]	0.53 ± 0.16[a]
Extracted Elastin (C)	0.59 ± 0.11*	119 ± 11*	0.24 ± 0.04*	1.05 ± 0.37[a]
Native Carotid (L)	0.95 ± 0.13*	105 ± 11*	0.20 ± 0.06*	2.39 ± 0.84*
Native Carotid (C)	2.59 ± 0.31*	125 ± 15*	0.41 ± 0.09*	5.72 ± 0.79*

Figure 6.

Mechanical properties of the electrospun prTE scaffolds. **(Top)** Representative stress-strain curves of electrospun prTE, extracted porcine elastin, and native porcine carotid arteries. **(Bottom)** Table of mechanical properties including ultimate tensile strength (UTS), percent elongation at failure, and elastic moduli of electrospun prTE compared to extracted porcine elastin and native porcine carotid arteries. The UTS and elastic moduli of electrospun prTE were not significantly different from the extracted elastin in the longitudinal direction. Note: [a]indicates no significant difference (ANOVA, Tukey post hoc, $p > 0.05$), compared to electrospun prTE in the same orientation, *indicates a significant difference (ANOVA, Tukey post hoc, $p < 0.05$) for comparisons to electrospun prTE in the same orientation, and **indicates $p < 0.01$, t-test.

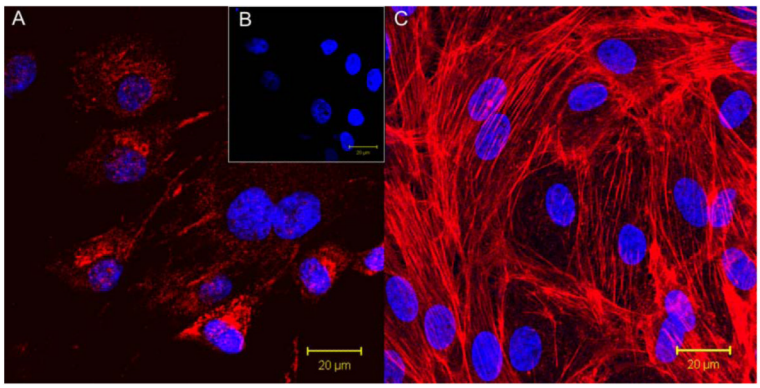

Figure 7.

(A) BMEOCs stained for vWF (red) with a DAPI (blue) nuclear stain. **(B)** Control for vWF stain with the DAPI nuclear stain. **(C)** Endothelial cell monolayer on 15 wt% prTE after 48 hours in culture. Nuclei are stained with DAPI and the cytoskeleton (f-actin) is stained with rhodamine phalloidin (red). BMEOCs attached and spread on the prTE scaffold.